Engineering and Technology Journal
Journal homepage: https://etj.uotechnology.edu.iq

# Experimental Study Convection Heat Transfer Inside the Triangular Duct Filled with Porous Media

**Sabah R. Mahdi*, Suhad A. Rasheed**

Mechanical Engineering Dept., University of Technology-Iraq, Alsina'a street, 10066 Baghdad, Iraq.
*Corresponding author Email: 21985@student.uotechnology.edu.iq

## HIGHLIGHTS

- Convection heat transfer is enhanced significantly in a triangular channel filled with a porous material.
- The average heat transfer coefficient increases with decreasing porosity compared to an empty triangular channel.
- The average Nusselt number decreases when using porous packed channels but increases with increasing porosity.
- Static pressure difference increases with increasing both Reynolds number and porosity.
- Empirical correlation is derived by relating the Nusselt number to the Reynolds number for the triangular porous packed channel.

## ARTICLE INFO

**Handling editor:** Sattar Aljabair

**Keywords:**
Force convection; Local Nusselt Number; Heat transfer coefficient; Porous media.

## ABSTRACT

Convection heat transfer inside an empty triangular channel when filled with porous media heated proportionally with a constant heat flux (1300 W/m²) at the Reynolds number range (3165- 10910) with packed beds has been studied. The present work investigates porous media experimentally. The packed duct has a length (1 m) and (0.1 m) hydraulic diameter packed with porous material made from spherical glass particles of two different diameters (5 mm, and 10 mm). The value of porosity for the channel is (0.468,0.616 and), respectively. This research studies the effect of changing the Reynolds number and porosity on the enhanced heat transfer coefficient and local Nusselt number. The results indicated that using a porous structure enhanced the convection heat transfer coefficient significantly by (90.2%) and (92.1%) at porosity (0.616, 0.468), respectively, when compared with an empty duct. The results also revealed that the local Nusselt number decreased when the flow's axial position increased with increasing air velocity. The pressure on both ends of the test section increased as the air velocity rose and reduced as the size of the glass spheres increased. Therefore, the drag coefficient decreases as the modified Reynolds number increases with the diameter of glass spheres. The current research was compared with previous research, and the results were satisfactory. Correlational relationships were reached between the Nusselt number and the Reynolds number.

## 1. Introduction

The porous medium is used in many fields and applications. It has been applied in industry, geology, and nuclear power. It also plays a key part in heat transfer and saving energy, such as Granular or porous insulators and high-power electrical file structures [1,2]. The porous medium is also applied in buildings and as insulating materials in nuclear reactors, dryness, and solar energy storage [3]. The methodology of fluid flow in a porous channel, which is based on the momentum equation or the power balance on this substance, has been mathematically summarized and interpreted in various experimental results (Darcy law). The rate of fluid velocity in a duct filled with highly permeable media is directly proportional to the pressure along the channel and inversely proportional to the fluid viscosity, according to this equation [4]. Due to the various technical applications that rely on the usage of porous material, it was necessary to investigate the heat transfer performance inside the porous channel. Porous media are used for both conduction and convection heat transfer.

The thermal conductivity of both the fluid and solid parts of the porous medium and the architecture of the porous media network determines the heat transport through a homogeneous porous medium. Because the porous material and the fluid are different phases with various thermal conductivities, one must express an equivalent thermal conductivity for both phases, referred to as effective thermal conductivity [5].Leung et al. [6] studied the heat transfer experimentally inside a horizontal isosceles triangular duct. The investigations were performed to study the effect of corner geometry on forced convection inside a triangular duct having sharp corners with five different apex angles (θa=15°, 30°, 40°, 60°, and 90°). The triangular compact



http://doi.org/10.30684/etj.2022.136144.1297
Received 24 September 2022; Accepted 01 November 2022; Available online 02 December 2022
2412-0758/University of Technology-Iraq, Baghdad, Iraq

heat exchanger was simulated using an electrical heating triangle duct. The isosceles triangle ducts were made of duralumin and had the same length (2.4 m) and hydraulic diameter (0.44 m). The investigation was performed under turbulent flow with Reynolds number range ($7000 \leq ReD \leq 20000$). It was found that the best thermal performance is achieved with an apex angle of (60°).

Hesham et al. [7] Investigated the forced convection heat transfer experimentally for a pulsating flow inside a horizontal hot cylinder partially filled with porous media. The horizontal test cylinder is made of copper (38) mm in diameter and (1) m long. The experimental work was performed for a laminar water flow inside the cylinder as a steady and pulsating flow with different frequencies. Carbon steel balls with (6.35 mm) diameter were used as particles, filling the tested cylinder, and the porosity (Ɛ) of the porous media was determined experimentally and found to be (0.4). The operating parameters range was considered; for Reynolds number from 400 to 2000, heat flux from (10 kW/m$^2$ to 60 kW/m$^2$) and pulsation frequencies from zero up to 5 Hz for different filling ratios from zero to unity. The obtained experimental results showed that for the considered range of the operating parameters, the Nusselt number and the heat transfer coefficient increase with increasing Reynolds number for a steady and pulsating flow. Nusselt number increases with increasing filling ratio with porous media for steady but pulsating flow. Nusselt number for pulsating flow is more significant than a steady flow.

Mortazavi and F. Hassan pour [8] numerically studied forced convection in a porous triangular channel. The flow was assumed to have constant properties. The flow was completely developed and laminar, and the conditions were maintained by a constant heat flux. The effects of porosity and permeability, the friction factor, the Reynolds number, and the Nusselt number on the air velocity and temperature distribution in a triangular channel were presented using accurate analytical solutions. The results show that the temperature profile exhibits the greatest difference in the maximum permeability and lowest porosity. With increasing porosity, both the friction factor and the Nusselt Number rise.

Fadhl et al. [9] The experimental results of the forced convection heat transfer and pressure decrease across a square packed duct (12.5x12.5x100 cm) were reported. The pad comprised 48 metallic wrapping coil units with a porosity of 0.98 and a thermal conductivity of (26 W/m.°C). For heat flux (0.56 to 2.73 kW/m$^2$), Reynolds number (40339 to 54797), and three boundary conditions of heat flux imposed on the duct surface, the local surface duct temperature, and local heat transfer coefficient distribution, Nusselt number, pressure drop, and friction factor were determined. Nusselt number rises in tandem with Reynold's number and heat flux. The packed duct's Nusselt number should be (1.21) times greater than the clear channel.

Jaber et al. [10] presented a research study on free. They forced convection heat transfer for three-dimensional laminar steady flows in a glass cubic box with dimensions of (30x30x30 cm) filled with porous medium. Plastic balls were a porous medium with a uniform diameter (11.7 mm). While an electrical heater heats the lowest wall, and the remaining walls are thermally isolated. Two vents with similar dimensions (6x6) cm with length (70 cm) constructed of clear plastic for air entering were made at the two vertically opposite walls, one for input and the other for air exit. The investigation of the porous media influence on the forced convection heat transfer with the selected heat flux values and for the ($Re_{PM}$) Reynolds number range (17.45 - 22.13) for every heat flux was included in the experimental work. For the average Nusselt number ranges (41.52 - 82.85), air enters from the bottom and escapes from the top in this experiment. According to the results, the average Nusselt number rises as the Reynolds number rises and falls as the high heat flux rises.

Seyed Soheil Mousavi and Mohammad Nikian [11] presented the first research to provide an exact analytical solution for convection heat in a triangular duct. The closed dimensionless temperature, the Nusselt number, and dimensionless temperature, as well as the center of the cross-section, were calculated using the finite series expression method. The authors believe that the proposed solution method could be applied to similar problems, such as heat convection in non-equilateral geometry, finding solutions for other thermal boundary conditions, and modeling the effect of heat dissipation in triangular ducts.

Varun et al. [12] stated that the duct geometry significantly impacts heat transfer in both laminar and turbulent flow conditions. This paper summarizes the findings of various triangular duct studies. This article looks at natural and forced convective heat transfer using Newtonian fluids, both experimentally and numerically. Compared to all other boundary conditions, the optimum heat transfer occurs under axially uniform wall heat flux with peripheral uniform wall temperature boundary conditions. Furthermore, rounding corners improve heat transfer and increase pumping power, which is directly related to operating costs. The result is that a triangle cross-sectional duct has the lowest friction factor compared to other arbitrary cross-sectional ducts. Also, the friction factor is inversely proportional to the Reynolds number in the fully developed region and becomes independent of flow direction distance.

Rafel et al. [13] tested the convection heat transfer in three channels (triangular, cylindrical, and rectangular) sectional area of (1 m) test reg and a (0.1 m) hydraulic diameter packed bed (ball glass having d=12 mm) in an experimental environment with a steady heat flux (1070 W/m$^2$) and Reynolds numbers in the range of (12461-2500). The effect of varying the Reynolds number and duct geometry on the temperature profile and local Nusselt number was demonstrated. The wall temperature along the channel drops when the Reynolds number rises with the same heat flux in a comparison of three ducts. As the Reynolds number rises, the average Nusselt number rises as well. The triangular channel's local surface temperature is more than that of the rectangle channel, which is higher than that of the cylindrical channel. The void fraction of the triangular channel was higher than that of the rectangle and cylinder channels. The test rig's length and hydraulic diameter are the same, and the local Nusselt number reduces as the length of the duct rises. The local Nusselt number of the triangular channel is also higher than the rectangle and cylinder ducts.

R. Kumar et al. [14] Investigations of five different duct models to analyze how changing the corners affects the heat transfer and friction factor. The first has a traditional triangular channel with small corners, while the remaining four structures have a variety of rounded corner duct combinations. Furthermore, the final model (Model-5) has a rounded corner with dimple protrusions on the heat-conducting side. Compared to a conventional duct with Reynolds numbers of 17500 and 3600, the

Nusselt number and friction factor increased by 191 percent and 287 percent, respectively. As a result, improved performance, rounded corners, and roughness are recommended through the triangular channel.

Mahdi et al. [15] presented an experimental study of flow and heat transfer behaviors in a rectangular duct with porous media and air as turbulent flow's working fluid entry length. The rectangular duct (300 mm x 30 mm) with a hydraulic diameter of (54.54 mm) was subjected to a constant lower surface heat flux ($1.5x10^2$-$1.8x10^2$ w/$m^2$), with a Reynolds number ranging from ($3.3x10^4$ to $4.8x10^4$). Copper mesh inserts (as porous media) with a diameter of 54.5 mm are considered for various distances (10 mm), (15 mm), and (20 mm) between two adjacent screens in the porosity range (0.98 - 0.99) for experimentation. The impact of the porous height ratio was also considered (full and partial). It was found that using mesh inserts improves the heat transfer by a factor of (2.2) times compared to a plain surface.

Hikmat N. Abdulkareem et al. [16] studied the forced convective heat transfer experimentally in a vertical channel packed with a spherical porous medium heated with constant heat flux. The channel was covered with a spherical glass of three different diameters (1, 3, and 10 mm) in the range ( 0.0416 < (particle diameter / inner channel radius). The experimental setup included a packed bed assembly made of a copper tube with a (48 mm) inside diameter, (54 mm) outer diameter, and (1150 mm) heated length and constant heat flux. Water flowed against gravity in the test section, which was vertically oriented. The result showed that raising the Reynolds number by 65 percent raised the local Nusselt number by 34 percent while increasing heat flux by 71 percent increased it by 11 percent. When the particle diameter is between 1 and 3 mm, the heat transfer rate increases, but it decreases when the particle diameter is between 3 and 10 mm. At 97 percent, pressure drops are minimal, while porosity rises by 23 percent.

Mohammed [17] used the Fluent CFD software to study the laminar natural convective heat transfer for air captured between an outer cold circular enclosure and a heated inner equilateral triangular cylinder. Gopal et al. [18] utilized the finite element analysis to investigate the unsteady free convection heat transfer in an enclosure with two heated horizontal circular cylinders under a magnetic field. Rehman et al. [19] also used finite element analysis to study the free convection heat transfer in a triangular porous enclosure embedded with a T-shaped fin, the left/right walls are designed cooled, and the top segments are adiabatic. Finally, Alshehri et al. [20] mathematically investigated the effects of the Darcy-Forchheimer flow of hybrid and single nanofluid blended in Kerosene Oil.

As presented above, it is obvious that convection heat transfer inside empty and packed ducts is well addressed and covered in various situations regarding the duct geometry and the shape and size of porous media. However, there are still few experimental studies concerning the convection heat transfer in a triangular channel packed with porous media at constant heat flux and changing the porosity. Therefore, the present work has been conducted to solve this problem.

## 2. Objectives of the Present Work

This study aims to perform an experimental investigation of the forced convection heat transfer in a triangular duct with and without porous media at a constant heat flux of 1300 W/$m^2$. The study covers the Reynolds number range (3165-10910) at two porosity values: 0.468 and 0.616, to estimate their impact on the temperature profile, heat transfer coefficient, Nusselt number, and static pressure difference. Also, it is intended to obtain an empirical correlation between the average Nusselt number and both the Reynolds number and porosity.

## 3. The Experimental Setup

An experimental rig was designed to study the heat transfer process by forced convection in a porous duct. Generally, the experimental apparatus shown diagrammatically in Figure 1 consists of the following assemblies:

1) Triangular channel.
2) Electrical heater
3) Porous media.
4) Air blower.

The total length of the channel is (1 m) with (0.1 m) hydraulic diameter and equilateral sides of (0.17 m), and it is manufactured from a galvanized sheet with a thickness of (1 mm). Its outer surface is insulated using rubber foam insulation material of (0.036 w/m. K) thermal conductivity to prevent any heat interaction with the surroundings to the heating process, as shown in Figure 2.

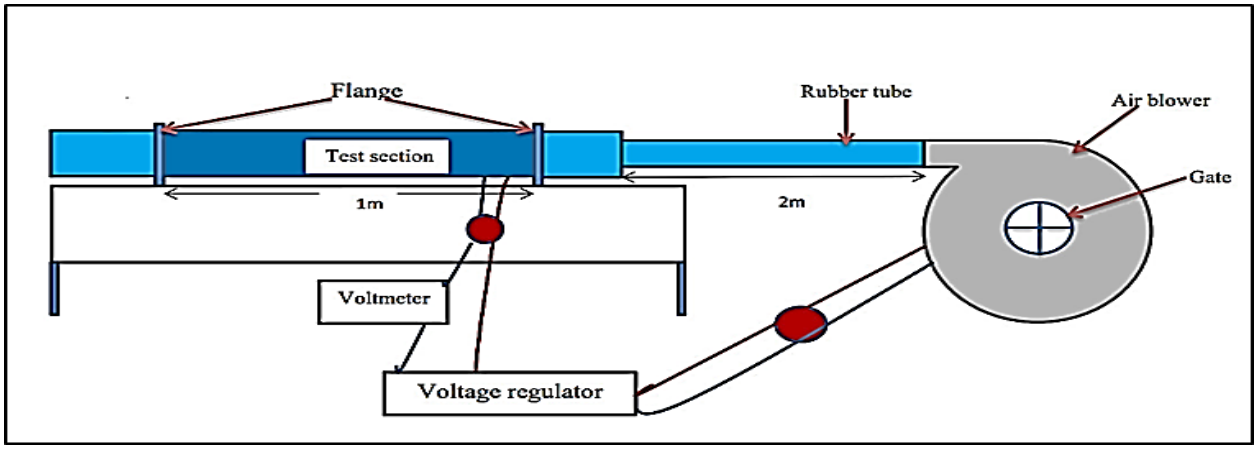


**Figure 1:** Schematic diagram of the experimental apparatus

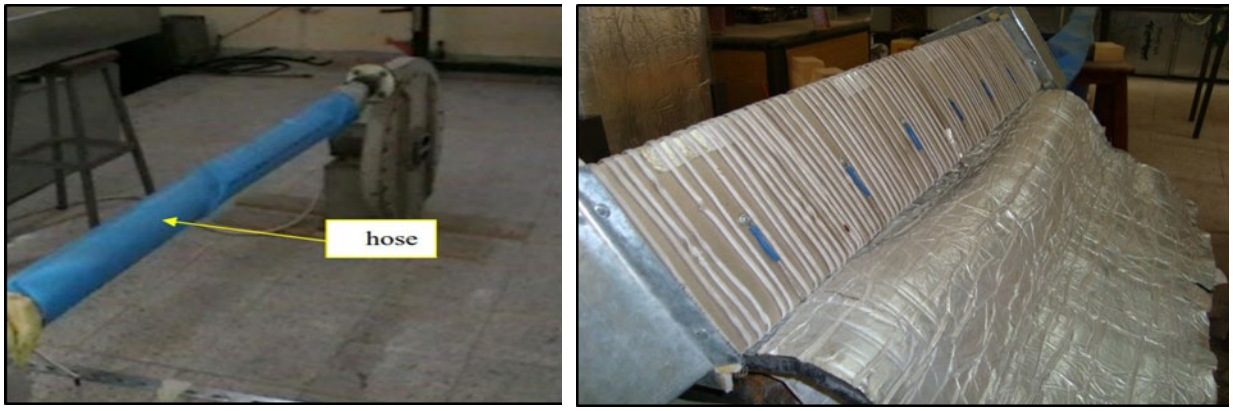


**Figure 2:** Flexible rubber tube (hose) and test duct

The air enters the triangular channel using an air blower, and a flexible rubber tube with a diameter of (10 cm) and a length of (2 m) connects the blower output to avoid vibration. The air blower is connected with the channel through a connection box manufactured with dimensions (20×20 cm and t=10 cm) and connected with the circular duct (D=0.1m, L=10 cm). In addition, another connection box (equilateral triangle) with dimensions (a=17 cm) and a mesh were placed at the channel to prevent the loss of particles from the outlet of air during the experiment.

Along the test rig, two electric heaters produced a constant heat flux (1300 W/m$^2$). A voltage regulator provides the heater with AC to control the incoming voltage according to desired heat flux. The electrical heater is made of (Nickel-Chrome), and the resistance is (18.7 ohms) with a coil diameter (0.25 mm). The electric heaters were installed by warping the channel's outside surface 54 times. The two heaters were connected in series. The blower's structure with power supply by a 3 -phase, (1.12 KW), (2872 rpm), and (50) $H_{Z,}$ were utilized, and Figure (3a) shows the output pipe diameter (5 cm). Shatter was used to close the inlet blower gate, and five flow rate levels can be produced, Figure (3b).

**(a)**

**Figure 3:** (a) Air blower

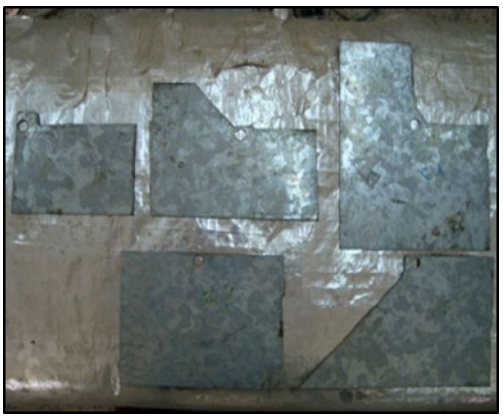

**(b)**

**Figure 3:** (b) Shatter

Two diameters (12 mm and 5 mm) of glass sphere as a porous medium were used to study the convection heat transfer in this work and fill the test section with it. First, the average diameter of a glass sphere was measured with an Electronic Digital

Vernier Calliper while the ball was clamped in it. Then, the parameters were measured by gripping the ball and spinning the sphere with the Vernier to ensure that it was spherical in shape and size, as shown in Figure 4.


**Figure 4:** Porous media

Thermocouple type-K (chromel – alumel) wires are used to measure the temperature in the apparatus, see Figure 5. Eighteen sensors were installed on the surface of the duct, the surface of the channel was divided into six sections, and every six sensors were installed in the face of the channel where the average of three sensors for the same point of each section was taken. In addition, two sensors were placed at the beginning and end of the test section to measure the air temperature. Thus, the total number of sensors used is twenty, see Figure 6. In addition, Arduino system type mega and Uno cart were used to record the system's temperature.

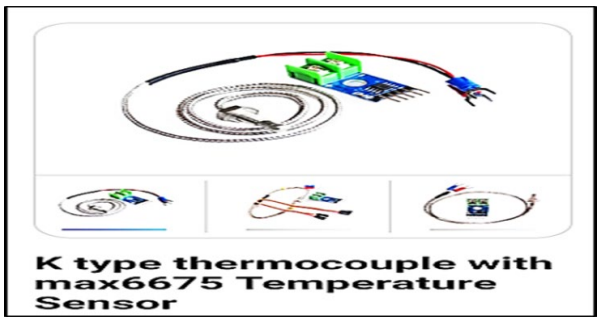


**Figure 5:** Thermocouple

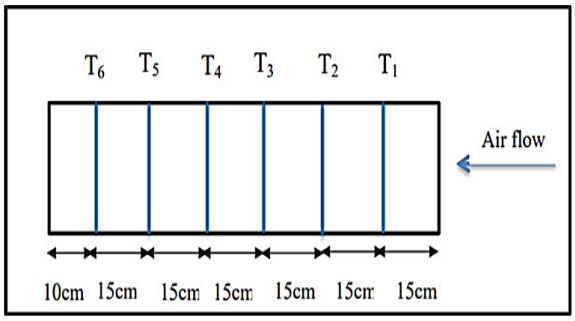


**Figure 6:** The distribution temperature along the duct surface within six sections

## 4. Experimental Calculation

The following relationships can be used to compute the average air temperature [16]:

$$Tb = \left(\frac{Ti+To}{2}\right) + 273.15 \quad (1)$$

The following relationship can be used to calculate the characteristics of fluid based on the average temperature [21];

$$\rho_f = 4.94 - 0.027\,\mathrm{Tb} + 6.5 * 10^{-5}\,\mathrm{Tb}^2 - 7.6 * 10^{-8}\,\mathrm{Tb}^3 + 3.41 * 10^{-11}\,\mathrm{Tb}^4 \quad (2)$$

$$\mu_f = 1.4 * 10^{-6} + 5.2 * 10^{-8}\,\mathrm{Tb} + 1.3 * 10^{-12}\mathrm{Tb}^2 - 3.4 * 10^{-13}\mathrm{Tb}^3 + 12.7 * 10^{-16}\mathrm{Tb}^4 \quad (3)$$

$$K_f = 1.51 * 10^{-16} + 8.9 * 10^{-5}\mathrm{Tb} + 2.9 * 10^{-9}\,\mathrm{Tb}^2 - 9.9 * 10^{-11}\mathrm{Tb}^3 + 8.6 * 10^{-14}\,\mathrm{Tb}^4 \quad (4)$$

$$\mathrm{Pr}_f = 0.78 - 1.09 * 10^{-4}\,\mathrm{Tb} - 1.37 * 10^{-6}\,\mathrm{Tb}^2 + 3.41 * 10^{-9}\,\mathrm{Tb}^3 + 3.1 * 10^{-12}\,\mathrm{Tb}^4 \quad (5)$$

$$Cp_f = 1.08 - .002\,\mathrm{Tb} + 3.79 * 10^{-6}\,\mathrm{Tb}^2 - 6.29 * 10^{-9}\,\mathrm{Tb}^3 + 4.17 * 10^{-12}\,\mathrm{Tb}^4 \quad (6)$$

The equal area approach was used to determine the average velocity of airflow through the test portion [22]. The following Equation was used to calculate the average air velocity at seven different locations:

$$u = \frac{v1+v2+v3+\cdots+v7}{7} \quad (7)$$

The mass flow rate (ṁ) for the air can be calculated by:

$$\dot{m} = \rho a * Ac * u \quad (8)$$

Where (Ac) is the duct's cross-sectional area. Convective heat transfer can be computed as follows [23]:

$$Q = \dot{m} * Cp_f * (T_o - T_i) \quad (9)$$

$$q = \frac{Q}{As} \quad (10)$$

Where (As) is the surface area for the duct. The following relationship can be used to determine the local heat transfer coefficient [23]:

$$hx = {}^{q}/_{\Delta T_x} \quad (11)$$

$$Where, \Delta T_x \text{ is } (Ts)_x - (Tb)_x \quad (12)$$

$$(Tb)_x = T_i + \frac{x}{L} (T_o - T_i) \quad (13)$$

(Ts)$x$ = The average of three surface locations in the duct's cross-section. The local Nusselt number was determined by using this relationship [12];

$$Nu_x = \frac{h_x D_h}{K_{eff}} \quad (14)$$

The total power provided to the duct can be determined as follows;

$$P_E = I * V_o \quad (15)$$

The following relationships can be used to calculate the heat losses from heated ducts [12];

$$Q_{losses} = P_E - Q \quad (16)$$

The Reynolds number was determined by using the equation below;

$$Re = \frac{\rho_a u_a D_H}{\mu_a} \quad (17)$$

Where, $D_H$ is the hydraulic diameter. The Reynolds number was determined based on particle size by using this relationship [12]:

$$Re_p = \frac{\rho_a u_a d_p}{\mu_a} \quad (18)$$

Where, $d_p$ is the particle bed diameter. The modified Reynolds number based on particle size was determined using the following relationship. [12]:

$$Re^* = Re_p/(1 - \mathcal{E}) \quad (19)$$

The following relationship was used to get the average Nusselt number: [12]:

$$Nu_{ave} = \frac{1}{L} \int_{x=0}^{x=1} Nu_x \, dx \quad (20)$$

This integration was calculated using the Trapezoidal rule.

$$\int_0^1 Nul \, dl = \frac{\Delta L}{2} [Nu_1 + 2Nu_2 + 2Nu_3 + \cdots Nu_n] \quad (21)$$

Where ΔL is the distance between two sections. The difference in static pressure on both ends of the test section is defined as:

$$\Delta P = g \, \Delta H \, [\rho_w - \rho_{air}] \quad (22)$$

The friction factor through the porous medium is defined as [13]:

$$f = \frac{\Delta P}{L} \frac{D_p}{\rho u^2} \frac{\mathcal{E}^3}{\mathcal{E}-1} \quad (23)$$

## 5. Validation Case

To validate the present work, the experimental results, as shown in Figure 7 for empty channel compared with the results obtained from Equation (24) A traditional expression for the calculation of heat transfer in a fully developed turbulent flow in smooth tubes is that recommended by Dittus and Boelter [15].

$$Nu = 0.023 * Re^{0.8} * Pr^{0.3} \quad (24)$$

Equation (24) is true for fully developed turbulent flow in smooth tubes (2500 Re 100000) for fluids with Prandtl values ranging from around (0.6 to 100) and considerable temperature variations between the wall and fluid conditions. Both studies have the same behaviors, and the error was found to be 3.74 % which is acceptable for practical consideration.

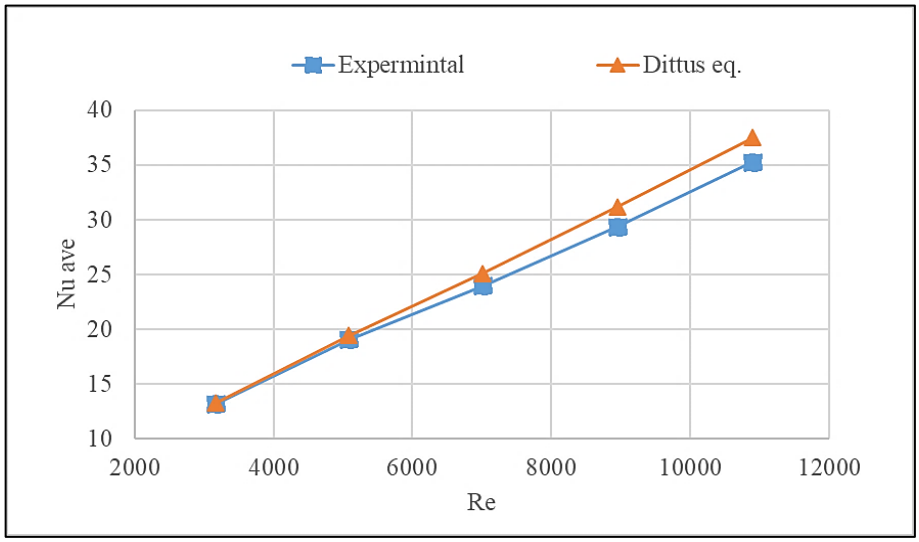


**Figure 7:** Validation case for empty channel

## 6. Results and Discussion

At different Reynolds numbers (3165 to 10915) with constant heat flux, the temperature distribution along the duct was measured. Figures 8 to 13 depict a direct reading of the axial distance temperature distribution for six average points fixed on the internal surface of the duct. The vertical axis is the difference in temperature of the sensor reading rate for the same point on the wall duct ($T_x$) and the supply air temperature (Ti), and the horizontal axis is the local position on the duct. Figure 8 shows the direct reading of the surface temperature profile along the empty channel, Figure 9 reveals the direct reading of the surface temperature profile for the channel at porosity (0.616), and Figure 10 displays the direct reading of the surface temperature profile for the channel at porosity (0.468) in different Reynolds numbers. The local wall temperature (Tx-Ti) in all ducts increases steadily with the axial location increasing and the air velocity increasing at the same heat flux. Therefore, the temperature of a surface duct with porosity (0.468) is more than that of a duct with porosity (0.616) which is more than in an empty duct.

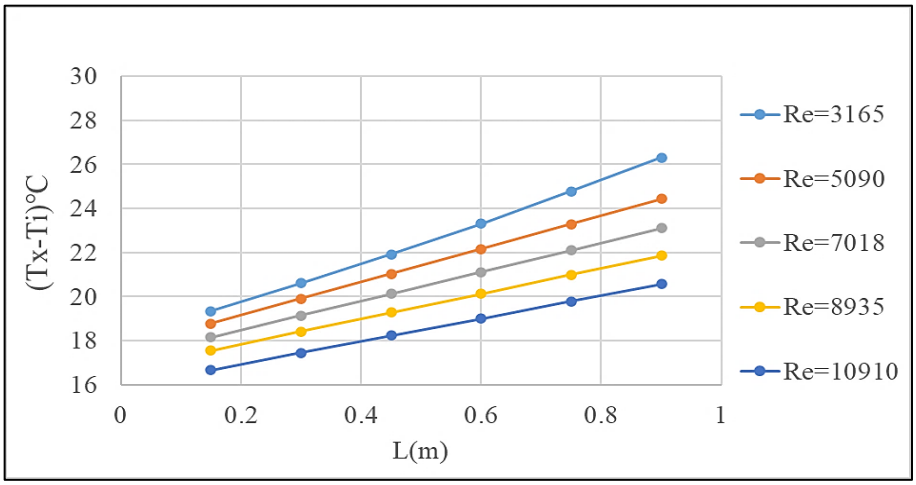


**Figure 8:** The local wall temperature empty duct in different Reynolds number

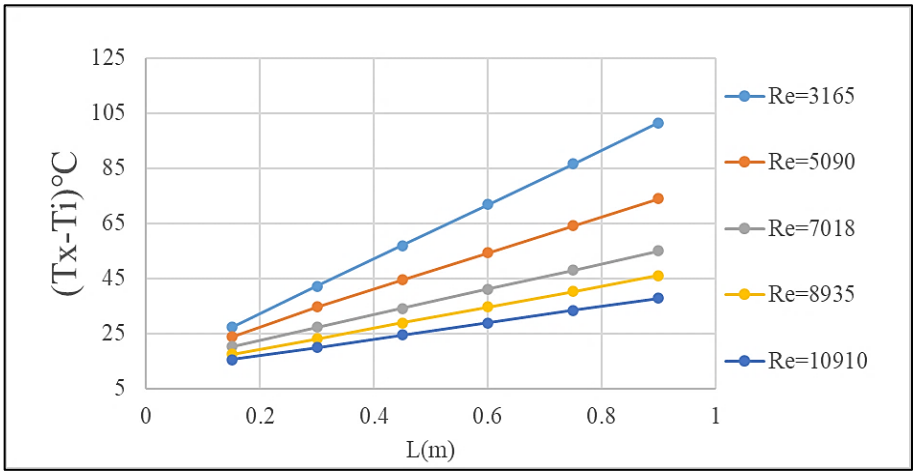


**Figure 9:** The local wall temperature for duct at (Ɛ=0.616) in different Reynolds numbers

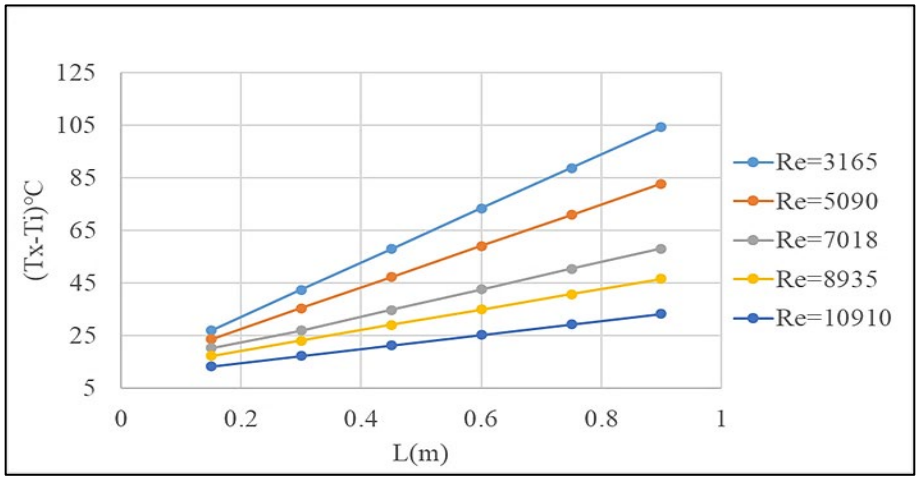


**Figure 10:** The local wall temperature for duct at (Ɛ=0.468) in different Reynolds numbers

Figures (11, 12, and 13) represent the effect of porosity change on the temperature distribution along the duct at (empty, Ɛ=0.616 and Ɛ=0.468). Each drawing is at a constant Reynold number (3165,7025, and 10915, respectively). It is noticed that the local wall temperature in the empty duct is first less. Then, it gradually becomes higher when filling the duct with a porous medium with a particle diameter of (12 mm), and finally rises when filling with (5 mm) particle diameter. But when the air velocity rises gradually, the temperature of the duct filled with the porous medium gradually decreases until the surface temperature of the empty duct becomes higher than the duct with the porous medium at high air velocities, see Figure 13. The reason is when the duct is filled with a porous medium, it will produce an air resistance that causes an increase in the pressure difference at both ends of the test section. As the porosity decreases, the air resistance rises. Therefore, the surface temperature of the duct increases.

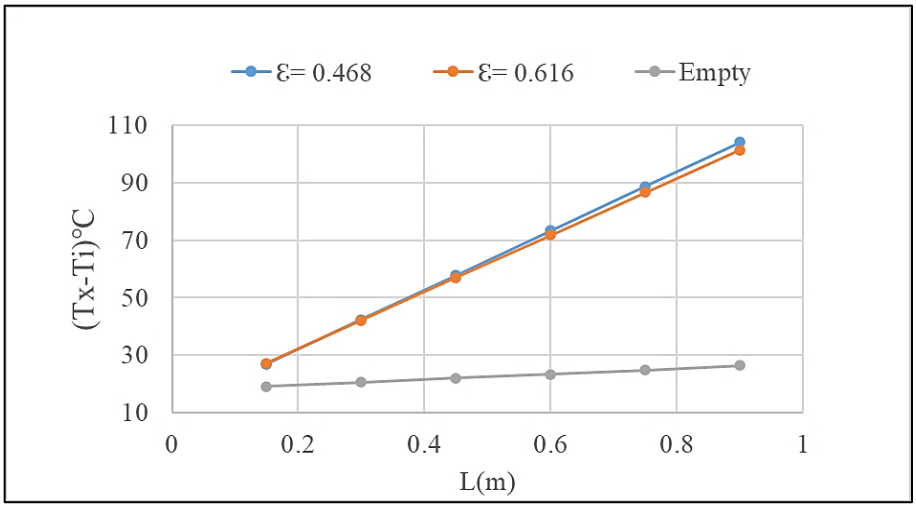


**Figure 11:** Effect of porosity change on the temperature distribution along duct at (Re =3615)

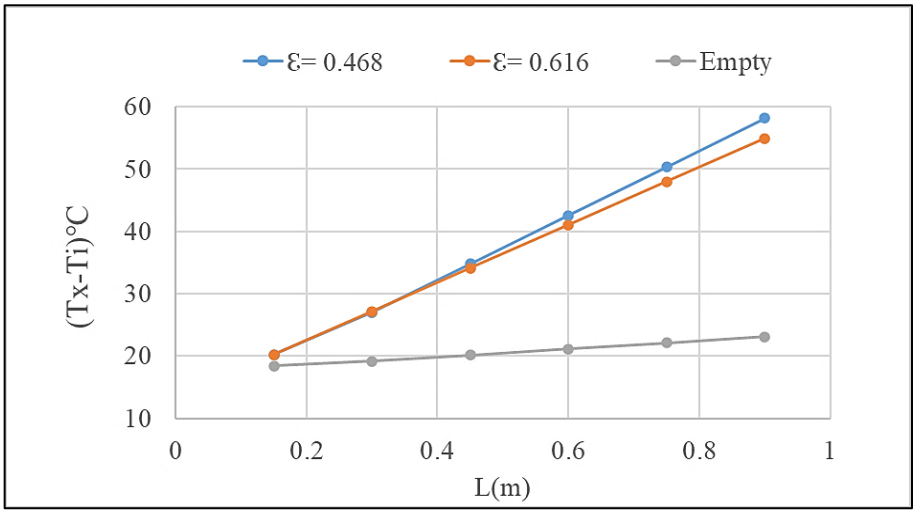


**Figure 12:** Effect of porosity change on the temperature distribution along the duct at (Re=7025)

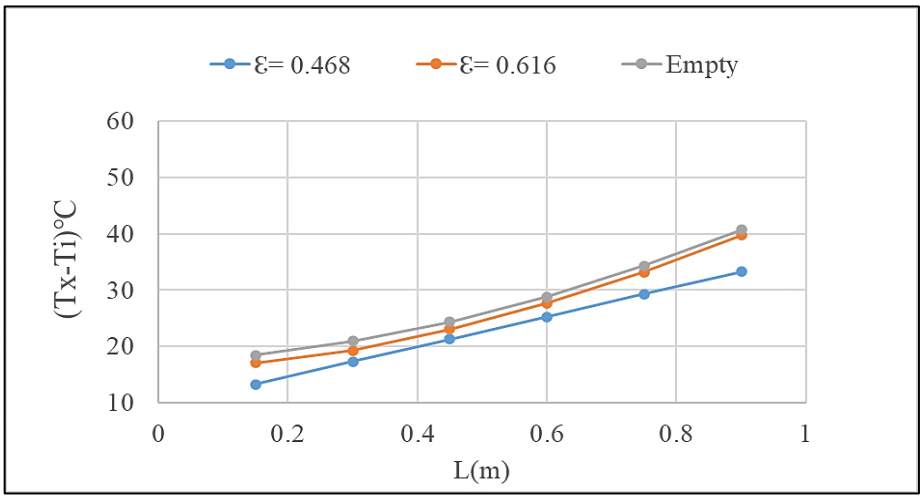


**Figure 13:** Effect of porosity change on the temperature distribution along duct at (Re=10915)

Figures 14 to 19 manifest the local heat transfer coefficient values in three channels (empty, at Ɛ=0.616 and at Ɛ=0.468) with different Reynolds numbers and constant heat flux ranges. It is higher in the channel at (Ɛ = 0.468), gradually lower at (Ɛ = 0.616), and much lower in the empty channel. It gradually decreases as the channel progresses towards the fluid flow because ($h_x = \boldsymbol{q} / (\boldsymbol{Ts}_x - \boldsymbol{Tb}_x)$), and the difference gradually decreases between the air temperature and the sensor reading rate for the same point on the duct wall ($Ts_x$-$Tb_x$) with increasing in axial position along the flow direction. The local heat transfer coefficient was higher at the highest Reynolds number.

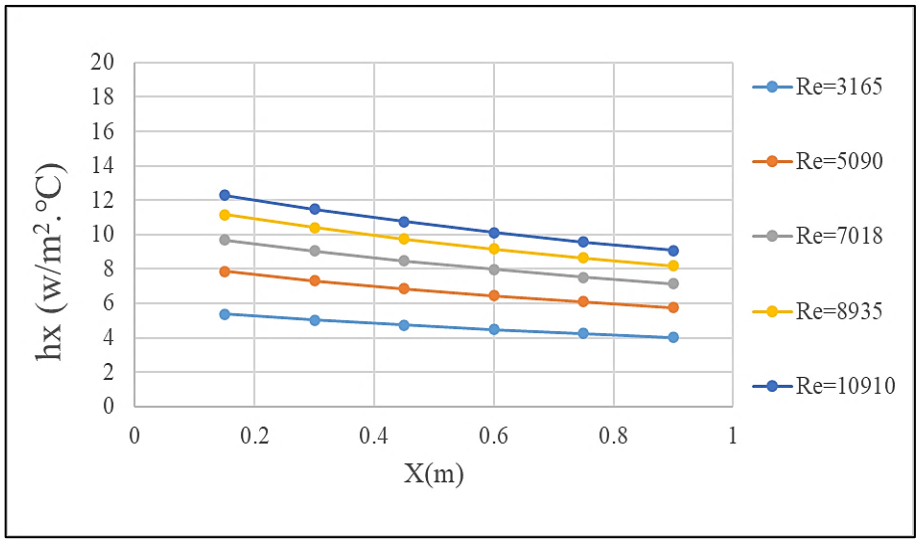


**Figure 14:** Effect of the air velocity change on the Local heat transfer coefficient along the empty duct

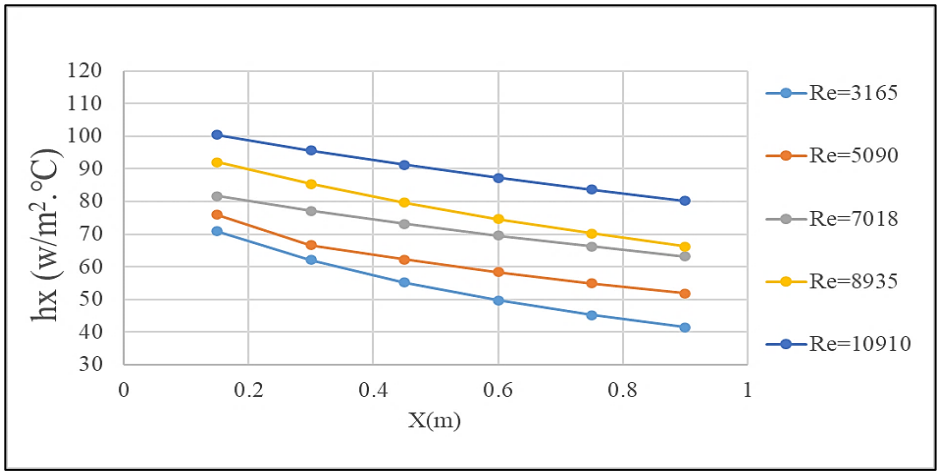


**Figure 15:** Effect of the air velocity change on the local Heat Transfer Coefficient for duct at (Ɛ=0.616)

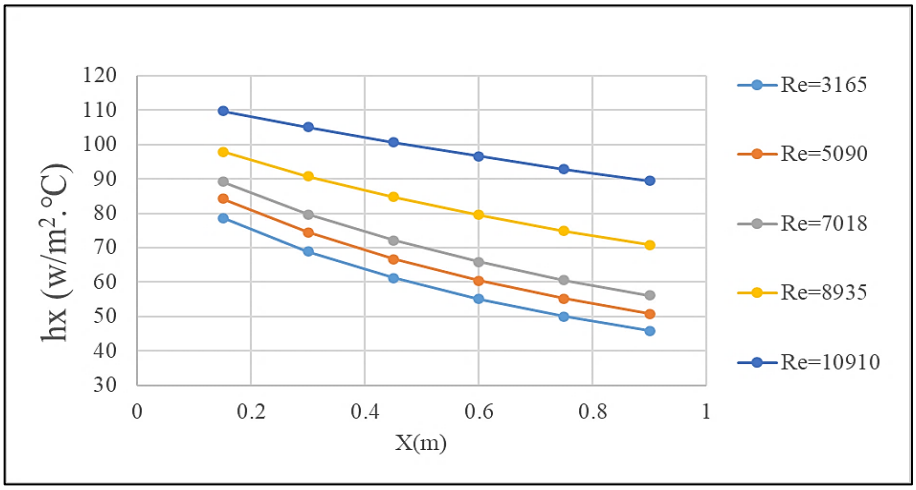


**Figure 16:** Effect of the air velocity change on the Local Heat Transfer Coefficient for duct at (Ɛ=0.468)

Figures 17 to 19 reveal the local heat transfer coefficient for three values of Reynolds number (3165, 7025, and 10915). It was higher in the channel at (Ɛ = 0.468), lower in the channel at (Ɛ = 0.616), and much lower in the empty channel. It gradually decreases as the channel progresses toward the fluid flow. Its value is higher at the highest air velocity, so the temperature gradually decreases for the same position on the duct wall, between the air and sensor reading rate ($Ts_x$-$Tb_x$). The difference between the air temperature and the reading of the sensors for the same point ($\Delta T_x$) is less at the channel at (Ɛ=0.468) and increases at the channel at (Ɛ=0.616) at the same point when air velocity increases.

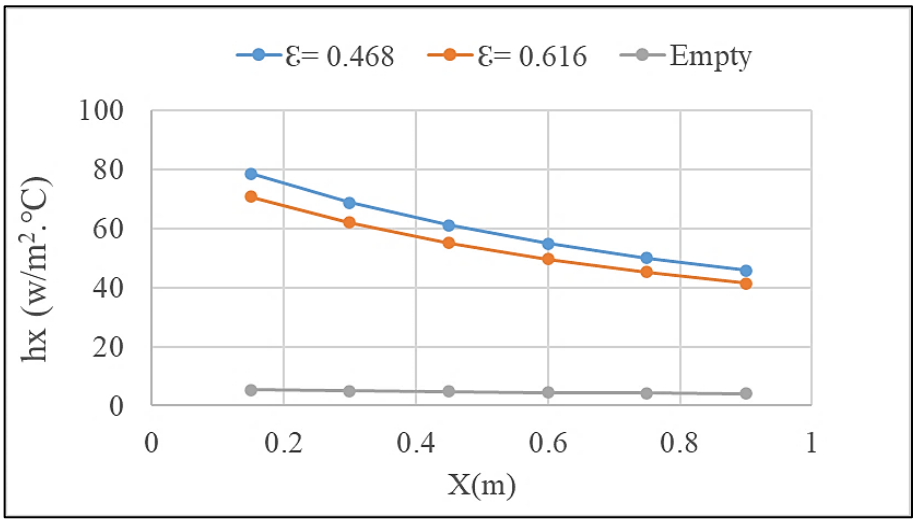


**Figure 17:** Local Heat Transfer Coefficient along the duct at (Re =3615)

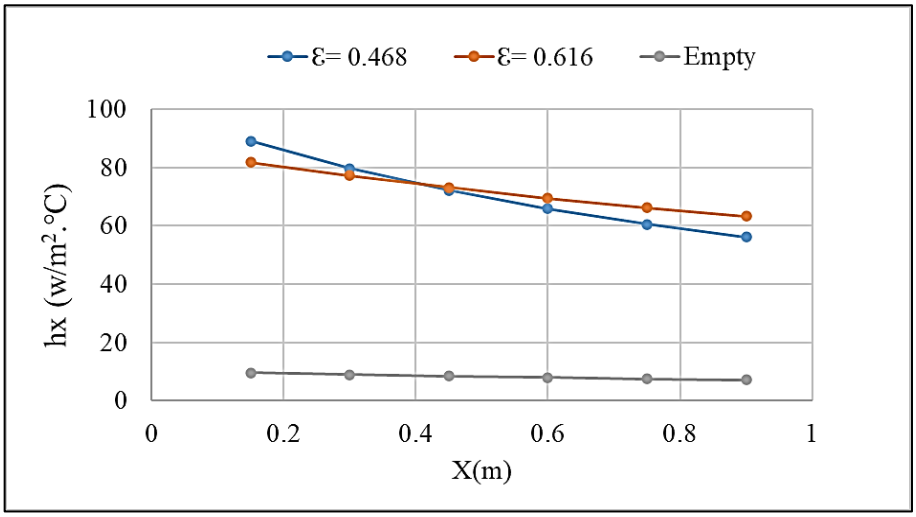


**Figure 18:** Local Heat Transfer Coefficient along the duct at (Re =7025)

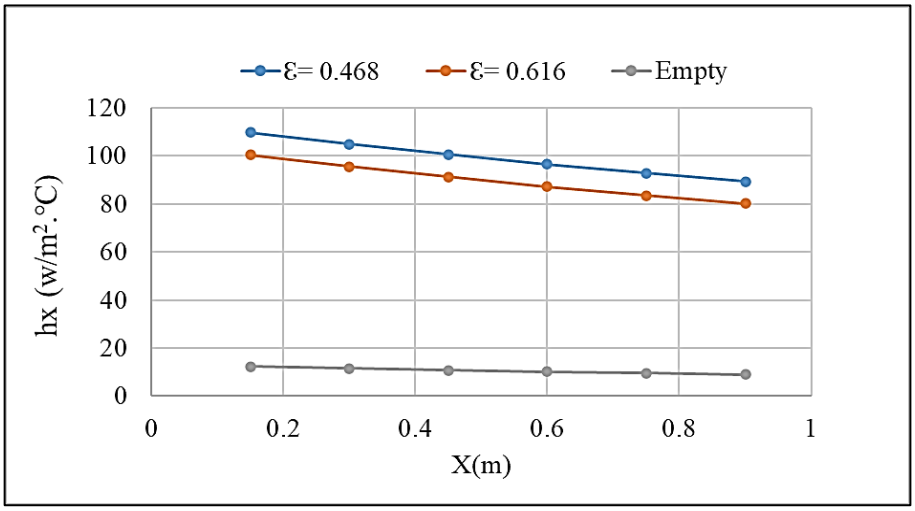


**Figure 19:** Local Heat Transfer Coefficient along the duct at (Re =10915)

Figure 20 elucidates that the average heat transfer coefficient in a duct at (Ɛ=0.468) is much more than for a duct at (Ɛ=0.616) and more than in an empty duct. Due to that, the difference of temperature in air and wall duct $(Ts-Tb)_X$ at the empty channel was substantially greater than in a channel at (Ɛ=0.616), which is more than in duct at (Ɛ=0.468). As a result, the average heat transfer coefficient percentage increased by about 92% at (Ɛ=0.468) and 91% at (Ɛ=0.616) compared with the empty duct.

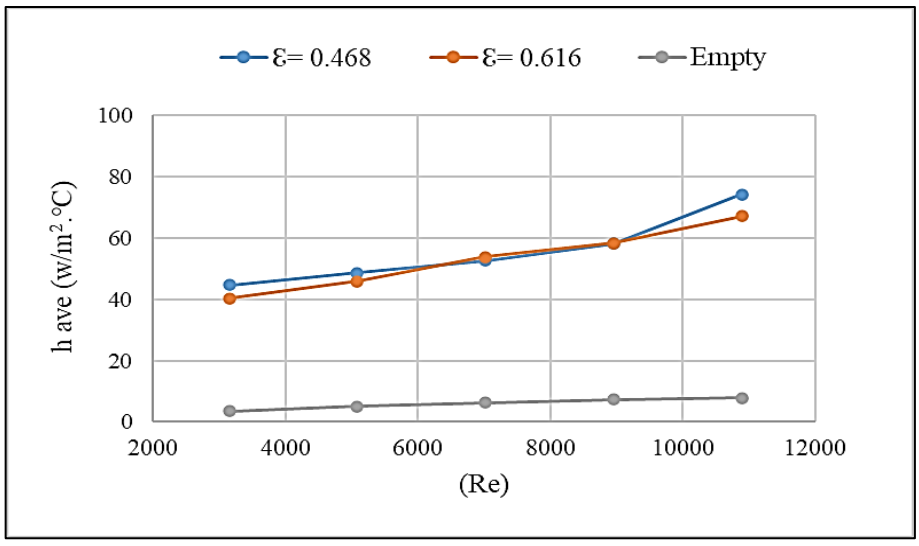


**Figure 20:** Average Heat Transfer Coefficient at duct {empty, (Ɛ=0.616) and (Ɛ=0.468)} with variation in Re (3165-10915)

The average Nusselt number rises with constant heat flux as the Reynold number rises. Because of the small difference in temperature between the air bulk temperature and the temperature of the wall duct, the average Nusselt number has a high value. Also, the average Nusselt number rises when the porosity rises because the effect of conduction decreases the effective thermal conductivity ($k_{eff}$) and the convectional heat transfer between the air and the hot channel wall, as well as with glass spheres, rises, Figure 21, shows that. The correlational, experimental relations of present work between the average Nusselt number and Reynolds number are $Nu = C\,Re^{M}$

$$Nu = 0.2266\,Re^{0.5152} \quad for\ (\mathcal{E} = 0.468) \quad ,Re\ (3195 - 10958) \tag{25}$$

$$Nu = 0.1447\,Re^{0.5298} \quad for\ (\mathcal{E} = 0.616) \quad ,Re\ (3180 - 10923) \tag{26}$$

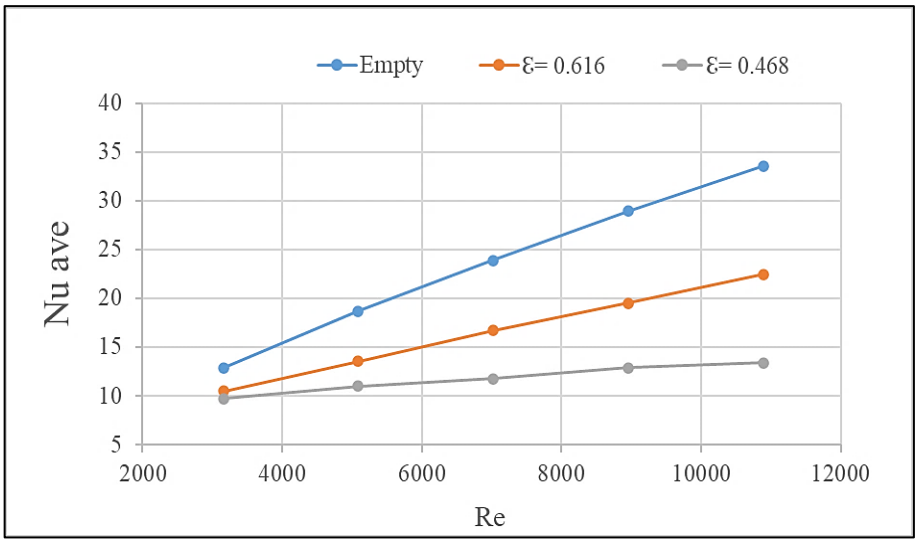


**Figure 21:** Average Nusselt number at duct empty, (Ɛ=0.616) and (Ɛ=0.468) with Re (3165-10915)

The comparison of the present result in local Nusselt number along the duct with porosity (0.616), Reynold number (3165), and inlet air temperature (27°C) with Rafel at duct with porosity (0.616), Reynold number (2500), and inlet air temperature (18°C) [13] are shown in Figure 22. The curves have the same behaviors with the error ratio between (2.8% - 4.5%).

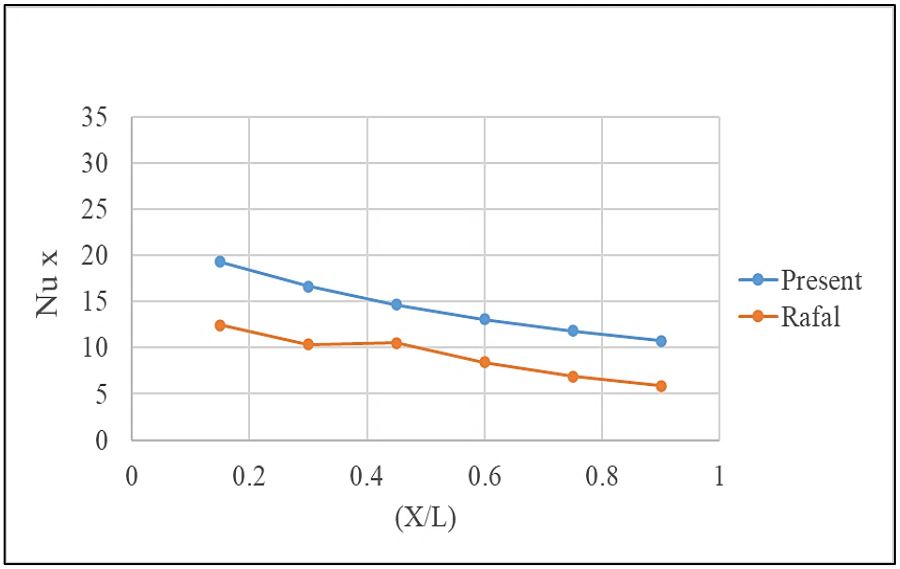


**Figure 22:** The comparison between the present work with previous literature Rafel [13]

The results showed that the difference in static pressure at both ends of the test section rises as the Reynolds number rises and falls as the porosity and diameter of the particle beads decrease, see Figures 23 and 24. Also, at constant porosity, the friction coefficient steadily drops when the modified Reynolds number rises, and as the particle size and porosity rise, it falls, as shown in Figure 25.

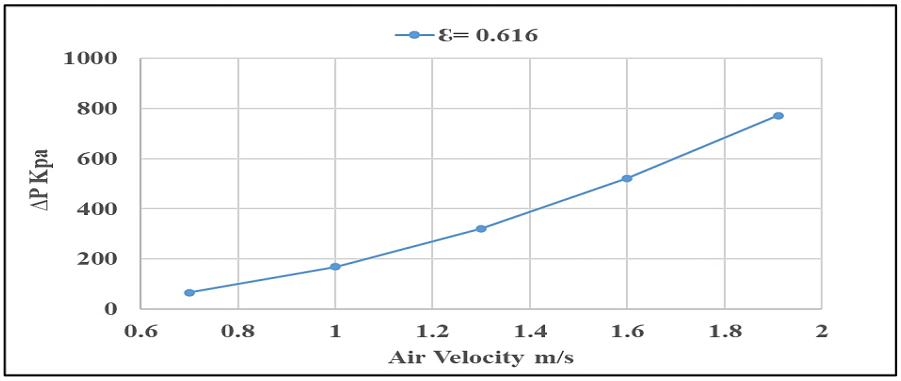


**Figure 23:** The pressure drops in the test section at (Ɛ=0.616)

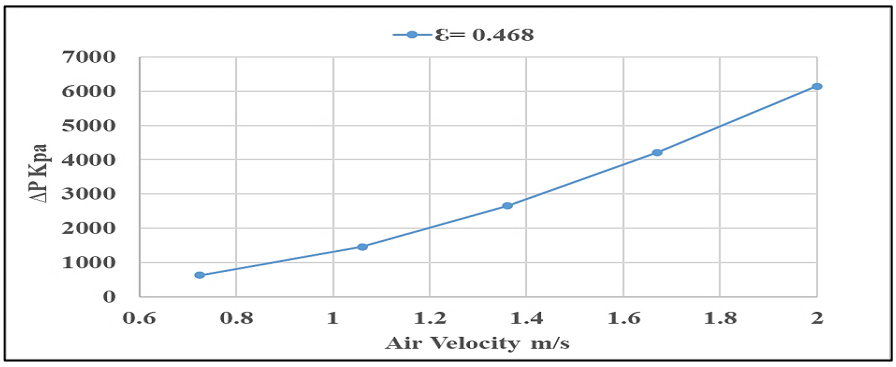


**Figure 24:** The pressure drops in the test section at (Ɛ=0.468)

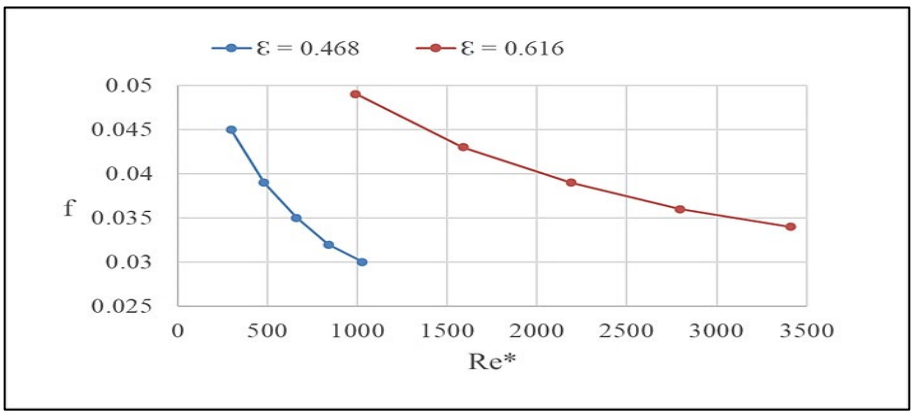


**Figure 25:** The friction factor in the channel at (Ɛ=0.616) and (Ɛ=0.468)

## 7. Conclusions

1) At constant heat flux, the local average temperature along the channel reduces when the air velocity rises. For the same Reynolds number, the local average temperature for the channel at (Ɛ=0.468) is more than in (Ɛ=0.616) which is more than in the empty duct, but when (Reynolds number > 10000), it becomes less in the duct which is filled with the porous medium.
2) The enhancement in the average heat transfer coefficient at Reynolds number (3165) was (90.2%) and (92.1%) at porosity (0.616, 0.468), respectively, when compared with the empty duct.
3) The average Nusselt number decreased when filling the duct with porous media because the ($k_{Eff}$) for porous channels was more than through the empty channel.
4) The difference static pressure on both ends of the test section increases with Reynolds number and porosity increase and with beads diameter decrease. This is due to the resistance in a packed bed from the viscous and turbulent forces.
5) The correlational, experimental relations of the present work were reached between the Nusselt number and the Reynolds number.

## Nomenclature

| Symbol | Definition | Units |
|---|---|---|
| A | Area | $m^2$ |
| Cp | Specific Heat Capacity | J/ Kg. K |
| h | Heat Transfer Coefficient | W / $m^2$ °C |
| hx | Local heat transfer coefficient | W / $m^2$ °C |
| ave | Average value | |
| I | Current | Amp |
| Vo | Voltage | Volt |
| k | Thermal Conductivity | W / m °C |
| K | Permeability | $m^2$ |
| Ɛ | Porosity | - |
| n | Number of Glass spheres | - |
| ΔP | The pressure drops in the test section | K pa |
| $P_E$ | Power | W |
| Q | Heat Transfer | W |
| q" | Heat Flux per unit area | W / $m^2$ |
| ṁ | Mass flow rate | Kg/s |
| $D_H$ | Hydraulic Diameter of duct | cm |
| d | Diameter of Glass sphere. | cm |
| Ti | Inlet air Temperature | °C |
| To | Outlet air Temperature | °C |
| Tb | Average air Temperature | °C |
| Ts | Surface duct Temperature | °C |
| Tx | The difference between the bulk air temperature and the sensor reading for the same point on the duct wall | °C |
| V | Volume | $m^3$ |
| u | Velocity of air | m/s |
| L | Length of the duct | m |
| Nu | Nusselt number | - |
| $Nu_X$ | Local Nusselt number | - |
| Re | Reynolds number | - |
| $Re_d$ | Reynolds number of particle diameter | |
| Re* | Modified Reynolds number | - |

### Author contribution

All authors contributed equally to this work.

### Funding

This research received no specific grant from any funding agency in the public, commercial, or not-for-profit sectors.

### Data availability statement

The data that support the findings of this study are available on request from the corresponding author.

### Conflicts of interest

The authors declare that there is no conflict of interest.

### Reference

**[1]** Kaviany, M, 1998, Principles of Heat Transfer in Porous Media,Chap.1-2, Second edition, the university of Michigan, America.

**[2]** Bejan, A. 2003. Convection Heat Transfer, Chap. 10, John Wiley and sons ins.

**[3]** Omar R. Alomar, Numerical Study of Inertia Effect on Natural Convection in A Horizontal Porous Cavity, M.Sc. Thesis., Mosul University, Iraq,2004.

**[4]** K. Vafai, and C.L. Tien Boundary and Inertia Effects on Flow and Heat Transfer in Porous Media, Int. J. Heat Mass Transf., 24 (1981) 195- 203. https://doi.org/10.1016/0017-9310(81)90027-2

**[5]** S. H. Rasheed, Mixed Convection Heat Transfer in Saturated Porous Media inside a Circular Tube, Ph.D. Thesis, University of Technology , Iraq,2006.

**[6]** C. W. Leung, T. T. Wong, H. J. Kang , Forced convection of turbulent flow in triangular ducts with different angles and surface roughness, Heat. Mass. Transf., 34 (1998) 63-68. https://doi.org/10.1007/s002310050232

**[7]** H. M. Mostafa, G. I. Sultan and M. G. Mousa, Heat Transfer for Pulsating Flow in a Horizontal Cylinder Partially Filled with a Porous Medium, Higher Technological Institute, Tenth of Ramadan City, Egypt ,Mansoura eng. j., 29 (2004) 34-43. https://doi.org/10.21608/bfemu.2020.132849

**[8]** S. Negin Mortazavi, Effect of Porous Media Properties on Heat Transfer in Triangular Porous Ducts with Iso-flux Walls, ASME 2011 International Mechanical Engineering Congress &Exposition IMECE2011, Denver, Colorado, USA. 10,2011 1017-1028. https://doi.org/10.1115/IMECE2011-65372

**[9]** K.H .Hilal, L.T. Fadhl, S.N. Faraj, Experimental Investigation of Heat Transfer and Pressure Drop in Square Metal Packed Duct with Different Boundary Heating, Eng. Technol. J., 30 (2012) 1082-1107.

**[10]** Hazim J. Jaber, Transfer in a partially Opened Cavity Filled with a Porous Media, Proceedings of International Conference on Engineering and Information Technology ICEIT,Toronto, Canada,2012.

**[11]** S. S. Mousavi, Mohammad Nikian, An experimental investigation on forced convection heat transfer of single-phase flow in a channel with different arrangements of porous media, Int. J. Therm. Sci.,134 (2018) 370–379. https://doi.org/10.1016/j.ijthermalsci.2018.04.030

**[12]** V. Goel, P. Guleria., R. Kumar, Effect of apex angle variation on thermal and hydraulic performance of roughened triangular duct, Int. Commun. Heat Mass Transfer., 86 (2017) 239–244. https://doi.org/10.1016/j.icheatmasstransfer.2017.06.008

**[13]** R. B. Smasem, Convection Heat Transfer in A Channel of Different Cross Section Filled With Porous Media, Kufa. J. Eng., 9 (2018) 57-73. https://doi.org/10.30572/2018/kje/090205

**[14]** R. Kumar ,Effect of Rounded Corners on Heat Transfer and Fluid Flow through Triangular Duct, J. Heat. Trans., 140 (2018) 121701. https://doi.org/10.1115/1.4040957

**[15]** A. N. Mahdi, Experimental Study of Forced Convection Heat Transfer Porous Media inside a Rectangular Duct at Entrance Region, J. Univ. Babylon. Eng. Sci., 27 (2019) 211–231. https://doi.org/10.29196/jubes.v27i1.1991

**[16]** H.N. Abdulkareem and K. H. Hilal, Convection Heat Transfer Analysis in A Vertical Porous,Tube Wasit J. Eng. Sci., 8 (2020) 31–45. https://doi.org/10.31185/ejuow.vol8.lss1.153

**[17]** A.A. Mohammed, Natural convection heat transfer inside horizontal circular enclosure with triangular cylinder at different angles of inclination, J. Therm. Eng., 7 (2021) 240- 254. https://doi.org/10.18186/thermal.849812

**[18]** G. C. Pal, G.Nammi, S.Pati, P. R. Randive, Laszl Baranyi, Natural convection in an enclosure with a pair of cylinders under magnetic field, Case Stud. Therm. Eng., 30 (2022) 101763. https://doi.org/10.1016/j.csite.2022.101763

**[19]** K. U.Rehman, W.Shatanawi, A. Taqi, M. Shatnawi, Case study on thermally fluidized suspension in porous enclosure: hybrid computational analysis, Case Stud. Therm. Eng., 30 (2022) 101730. https://doi.org/10.1016/j.csite.2021.101730

**[20]** A.Ahmed, Z. Shah, Computational analysis of viscous dissipation and Darcy-Forchheimer porous medium on radioactive hybrid nanofluid, Case Stud. Therm. Eng., 30 (2022) 101728. https://doi.org/10.1016/j.csite.2021.101728

**[21]** T. K. Salim, An experimental study for heat transfer enhancement by laminar forced convection from horizontal and inclined tube heated with constant heat flux, using two types of porous media,Tikrit J. Eng. Sci., 15 (2008) 15-36. https://doi.org/10.25130/tjes.15.2.09

**[22]** Eric M. Banks Christopher, Thesis. Airflow Traverse Comparisons using The Equal-Area Method, Log-Tchebycheff Method and the Log-Linear Method, NUCON International, Inc. Columbus, Ohio,2002.

**[23]** Holman, J. P., Heat transfer, 10th Edition, McGraw-Hill, 2009.